Analysis of air mass back trajectories with present and historical volcanic activity and anthropogenic compounds to infer pollution sources in the South Shetland Islands (Antarctica)

Danuta Szumińska* [1a], **Sebastian Czapiewski** [1b], **Małgorzata Szopińska** [2c], **Żaneta Polkowska** [2d]

[1] Kazimierz Wielki University, Poland
[2] Gdansk University of Technology, Poland

* **Correspondence:** Institute of Geography, Kazimierz Wielki University, Poland. E-mail: dszum@ukw.edu.pl

[a] https://orcid.org/0000-0001-7142-9080, [b] https://orcid.org/0000-0001-8010-1378, [c] https://orcid.org/0000-0003-2186-7781, [d] https://orcid.org/0000-0002-2730-0068

Abstract. This work analyses atmospheric transport of natural and anthropogenic pollution to the South Shetland Islands (SSI), with particular reference to the period September 2015 – August 2017. Based on data from the Global Volcanism Program database and air mass back trajectories calculated using the HySPLIT model, it was found that it is possible that in the analysed period volcanic pollution was supplied via long-range transport from South America, and from the South Sandwich Islands. Air masses flowed in over the South Shetland Islands from the South America region relatively frequently – 226 times during the study period, which suggests the additional possibility of anthropogenic pollution being supplied by this means. In certain cases the trajectories also indicated the possibility of atmospheric transport from the New Zealand region, and even from the south-eastern coast of Australia. The analysis of the obtained results is compared against the background of research by other authors. This is done to indicate that research into the origin of chemical compounds in the Antarctic environment should take into account the possible influx of pollutants from remote areas during the sampling period, as well as the possible reemission of compounds accumulated in snow and ice.

Introduction

Although Antarctica is the most isolated continent on Earth, it is influenced by global anthropogenic activity in its broad sense, and the effects of extreme natural phenomena (e.g. volcanic eruptions). This is mainly due to long-range atmospheric transport (LRAT) (Corsolini 2009; Cabrerizo et al. 2014). The presence of industrial, agricultural and volcanic compounds in Antarctica is explained by the phenomenon of global distillation (Corsolini 2009): contamination resulting from numerous evaporation and condensation processes may move to ever-higher latitudes (Bengtson-Nash 2011). This phenomenon is also known as the "grasshopper effect".

Since the 1960s, there has been an increase in the use of compounds classed as Persistent Organic Pollutants (POPs) in the Southern Hemisphere (Bargagli 2008), which has resulted in the presence of a wide range of pollutants in Antarctica. Hundreds of thousands of different industrial chemicals have been produced all over

the world, but only a proportion have been tested in the Antarctic environment (e.g. polychlorinated biphenyls [PCBs], the pesticides: methoxychlor, chlorpyrifos and dichlorodiphenyltrichloroethane [DDT], and polycyclic aromatic hydrocarbons [PAHs]), and the results of these studies are presented in review articles (e.g. Bargagli 2008; Corsolini 2009; Szopińska et al. 2016). However, in addition to industry, the combustion of biomass is a very important source of pollution in the Southern Hemisphere, mainly in the form of forest fires (Molina et al. 2015) and natural phenomena, such as volcanic eruptions (Dauner et al. 2015). These are above all a source of various forms of carbon (Edwards et al. 2006), including polycyclic aromatic hydrocarbons (Culotta et al. 2007; Fuoco et al. 2012; Kozak et al. 2017). Additionally, during volcanic eruptions metals such as mercury may also enter the atmosphere with dust. This type of research was carried out in the northern hemisphere after the eruption of Mount Etna in Southern Italy in 2001 and 2002 (Stracquadanio et al. 2003). However, to date, the impact of volcanic activity and forest fires in the Southern Hemisphere is still insufficiently known in Antarctica.

Regardless of the source of pollution (natural, and especially anthropogenic), these substances may pose a threat to the Antarctic ecosystem. The problem is the lack of well-developed detoxification mechanisms in Antarctic organisms (Bengtson-Nash et al. 2010). Moreover, polar ecosystems are very sensitive to the presence of pollution, which disturbs the equilibrium because of the close interconnections between individual elements of the environment. Both bioaccumulation of pollutants in the tissues of Antarctic organisms and bio-potentiation in the food chain may occur. This is particularly important for krill and penguins, whose occurrence is interdependent (Bengtson-Nash et al. 2010).

Therefore, it is extremely important to monitor pollutant concentration levels in the various elements of polar environments. No less important is also a detailed knowledge of the ways in which pollutants are transported to Antarctica. One such way is the aforementioned long-range atmospheric transport. Although the inflow of pollutants to the Antarctic is being limited by the range of circumpolar air circulation, the possibility of long-range atmospheric pollution has been indicated in some works (e.g. Lee et al. 2004; Mishra et al. 2004; Kallenborn et al. 2013; Cabrerizo et al. 2014). Therefore, the paper analyses the possibility of atmospheric transport of pollution to the South Shetlands. In addition, due to the still insufficient amount of literature data on this subject, particular attention is paid to the possibility of emissions of volcanic origin in the Southern Hemisphere.

Geographical background

Atmospheric circulation

Atmospheric circulation in the Antarctic Peninsula and the South Shetlands is driven by stationary lows near the Antarctic Peninsula and above the Bellingshausen and Weddell Seas bringing prevailing winds from NW and W to the South Shetland Islands (Kejna and Laska 1999). The second driver of air masses is migratory cyclones. Based on 15-year synoptic observations, Jones and Simmonds (1993) determined two mid-latitude branches of cyclone movement coming into Antarctica – from the Tasman Sea area and from around South America. Other authors (Simmonds and Keay 2000) have indicated that, over the period 1958–1997, cyclone density over the eastern Antarctic Peninsula has increased, in contrast to having decreased in the Antarctic Ocean. Moreover, based on numerous climatic works, Russel and McGregor (2010) summarised that atmospheric circulation patterns in the Southern Hemisphere have changed in the recent past, and this change is thought to have contributed to the warming trend observed in the Antarctic Peninsula over the last 50 years (*inter alia,* Vaughan et al. 2003; Turner et al. 2005; Vieira et al. 2008; Bockheim et al. 2013). Regardless of general warming, regional cooling has been observed in the Antarctic Peninsula since the end of the 20th century (Turner et al. 2016; Oliva et al. 2017). On the other hand, based on ice-core aerosol records, McConnel et al. (2014) associated the intensity of aerosol transport from industrial areas with the El Niño–Southern Oscillation. Long-range transport is recorded to be more vigorous in spring than

in other seasons. Moreover, the aforementioned authors observed multi-decadal changes in atmospheric transport, and suggested that regional-to-global scale circulation plays an important role in modulating aerosol concentrations and climate at multi-decadal timescales in the Antarctic region.

Volcanic activity in the Southern Hemisphere

Within the Southern Hemisphere there are areas of volcanic activity in the regions of South America, Antarctica, the South Sandwich Islands and New Zealand.

The western coast of South America is covered by plate-edge volcanism associated with continental drift leading to subduction of oceanic plates beneath the continental plate, transverse rift of the upper plate, fracturing of the plates, or subduction of the oceanic centre of spreading (Lara et al. 2013). The South American volcanic arc extends about 7,000 km from southern Chile to the south coast of Panama and is a zone of continuous subduction of the oceanic lithosphere of the Nazca plate beneath the South American continent.

The Antarctic continent and surrounding oceans constitute one of the world's largest Neogene volcanic provinces with the two main volcanic environments related to: 1) the West Antarctic Rift System (WARS); and 2) the northern Antarctic Peninsula volcanic field (Le Masurier et al. 1990). The first of these, a vast area of subglacial volcanoes, was described by Van Wyk de Vries et al. (2018) and includes 138 volcanic edifices, with particular concentrations in Marie Byrd Land and along the central WARS axis. In this region there are several volcanoes that have been active in historical times (Fig. 1A), including the Erebus volcano. The second is related to a crustal extension in the Bransfield Strait/South Shetland (Birkenmajer et al. 1986) and both submarine and subaerial volcanoes occur there (Fig. 1A). The most active volcano in this region is Deception Island, which is situated in the western sub-basin of the Bransfield Strait, just off-axis relative to the marginal basin-spreading centre (González-Ferrán 1991). The South Sandwich volcanic islands are the highest part of the intra-oceanic Scotia Ridge, which is located in the South Atlantic. Its origin is related to the steeply inclined

subduction of the South American plate beneath the Sandwich plate at a rate of 67–79 km/Ma (Leat et al. 2013).

Another volcanic region of the Southern Hemisphere is the New Zealand area, which has a particular continental plate collision system (Salmon et al. 2013). New Zealand is on the edge of the Pacific tectonic platform and the tectonic line that is the same fault that goes through Japan and the west coast of the United States (Jarmołowicz-Szulc and Kozłowska 2016). It runs along both the North and the South island, forming mountain ranges in both parts of New Zealand.

Within the analysed volcanic areas in the Southern Hemisphere there are 60 volcanoes whose activity is documented in historical sources (Table 1, Fig. 1). The majority (41) are associated with the western coast of South America. In terms of the number of years of documented volcanic activity (Table 1), the particularly active volcanoes of this area include: Calbuco, Copahue, Láscar, Llaima, Nevados de Chillán, Osorno, Planchón-Peteroa, Puyehue-Cordón Caulle, Sabancaya, San José, Tupungatito, Ubinas and Villarica. Of these, five were active in the period September 2015 to August 2017: Copahue, Láscar, Nevados de Chillán, Ubinas, Villarica, as was one volcano not listed above – Sabancaya. Volcanic activity was accompanied by, *inter alia*, emission of vapour, gases and dust of variable intensities, which rose to a height of 100–1,700 m above the volcanoes' summits, i.e. altitudes of about 3,000–7,000 m a.s.l.

In the research period, three volcanoes on the South Sandwich Islands were also active: Bristol Island, Saunders and Zavodovski (Table 1, Fig. 1). In the study period, ash plumes from these volcanoes moved towards the SE (May 2016) and SSW and SE (December 2016) (www.volcano.si.edu).

Of the volcanoes of the New Zealand region, only the White Island volcano was active in 2016 (Table 1, Fig. 1). In the Antarctic area the Erebus volcano on Ross Island was active in the study period. The activity of this volcano has been associated since 1972 with a continuous lava lake with steam plumes and occasional eruptions (Mattioli and LaFemina 2016).

Of the 61 volcanoes listed in Table 1, up to 40 were active in the 21st century and in most cases activity lasted for more than a year.

Material and methods

The potential for atmospheric transport via air masses to the South Shetland Islands from September 2015 to August 2017 (24 months) was examined. To verify the origin of air masses the HySPLIT model (The Hybrid Single Particle Lagrangian Integrated Trajectory Model) (Draxler and Rolph 2003; Draxler et al. 2009) was used to model 10-day back trajectories of air masses at 500 m a.s.l., 1,000 m a.s.l. and 2,000 m a.s.l., based on Global Data Assimilation System meteorological data. Simulations were prepared for the period from September 2015 to August 2017, with the South Shetland Islands being assumed as the destination point for air masses. In total, 731 air mass trajectories were determined. Then, the atmospheric transport trajectories were analysed, with a focus on those originating from remote areas that were potential sources of volcanic and anthropogenic pollution.

Moreover, the monthly frequency of air masses from selected directions was compared against monthly values of SAM (the South Annual Mode) and ENSO (El Niño 3.4) indices.

HySPLIT is used in the analysis of the propagation of air masses at given altitudes and to determine the possibility of substances propagating with these masses. Methods for modelling air mass trajectories are used, among others, in microbiology to track the spreading of fungal spores (Sadyś et al. 2015), anthropogenic pollution, including heavy metals (e.g. Chen et al. 2013) and PM10 and PM2.5 dusts (Shahid et al. 2016; Punsomponga and Chantara 2018), as well as in detecting desert dust masses (McGowan and Clark 2008; Escudero et al. 2011) and volcanic dust (Adame et al. 2015). The authors choose various trajectory intervals, from 3 to 10 days. Ten-day back trajectories have been used by, among others, Raga et al. (2016) in determining the origins of aerosols in mountaintop clouds in Puerto Rico.
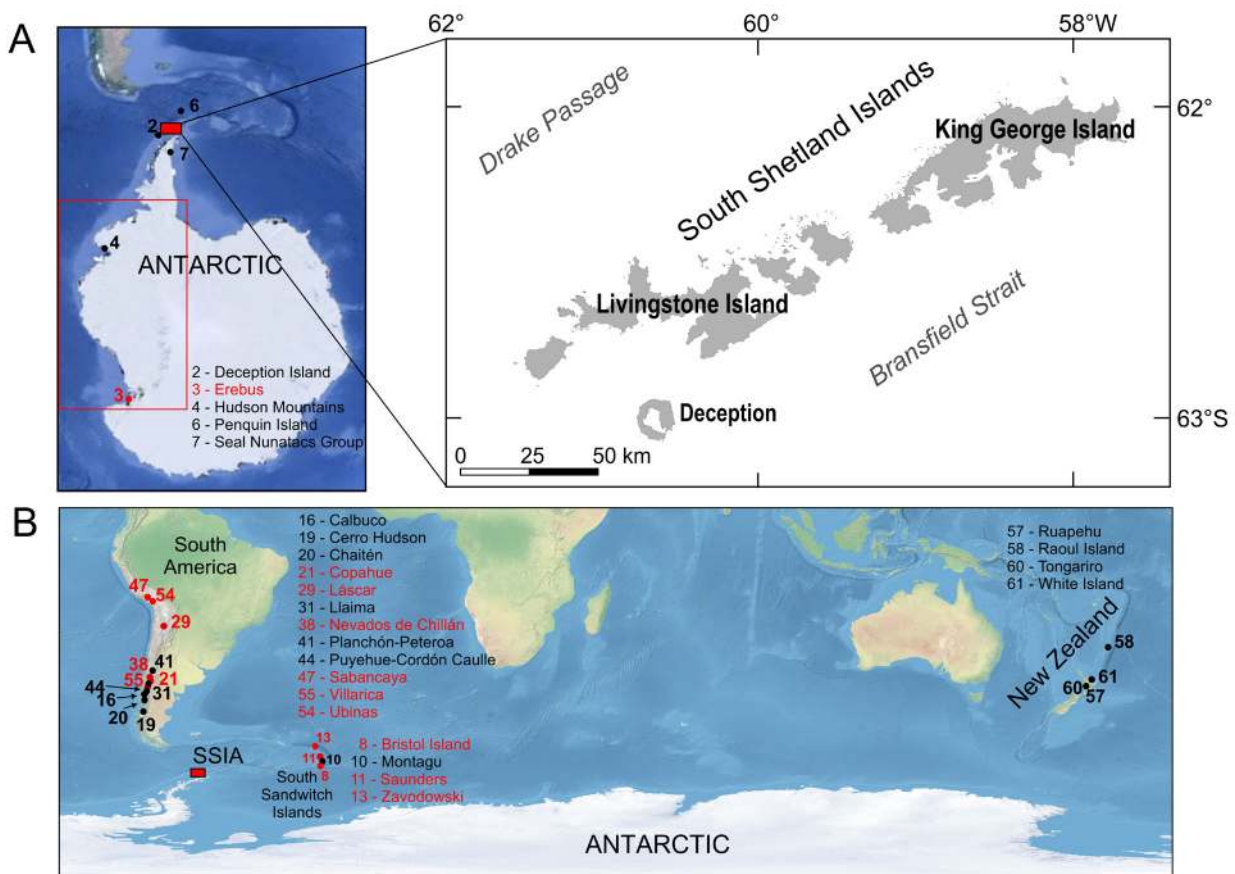

Fig. 1. Map of volcanoes: A – volcanoes in Antarctica active in the 20th and 21st centuries, B – volcanoes in South America, South Sandwich Islands and New Zealand active in 21st century. In red – volcanoes active from September 2015 to August 2017 (numbers of volcanoes according to Table 1) (based on: Global Volcanism Program, www.volcano.si.edu)

Table 1. Periods of volcanic activity in volcanic regions: South America, Antarctica, New Zealand to Fiji over the historical period (confirmed activity based on: Global Volcanism Program, www.volcano.si.edu). In bold red – volcanic activity in the period September 2015 to August 2017; in bold black – volcanic activity in the 21st century (names in alphabetic order)

No.	Name	Location	Coordinates	Elevation [m a.s.l.]	Periods of volcanic activity	Number of years with volcanic activity	Type
1	Buckle Island	Antarctic	66.78°S 163.25°E	1239	1899, 1839	2	Stratovolcano
2	Deception Island	Antarctic	63.001°S 60.652°W	602	1987[a], 1972[a], 1970, 1969, 1967, 1912,1871[b], 1842, 1839[a], 1827, 1800	11	Caldera
3	Erebus	Antarctic	77.53°S 167.17°E	3794	16.12.1972–24.08.2017 (continuing lava lake existence with steam plumes and occasional eruptions) 1972, 1963, 1955, 1947, 1915, 1912, 1911, 1908, 1903, 1841	55	Stratovolcano
4	Hudson Mountains	Antarctic	74.33°S 99.42°W	749	1985[a]	1	Stratovolcano (es)
5	Melbourne	Antarctic	74.35°S 164.7°E	2732	1892	1	Stratovolcano
6	Penguin Island	Antarctic	62.1°S 57.93°W	180	1905[c], 1850, 1683[c]	3	Stratovolcano
7	Seal Nunatacs Group	Antarctic	65.03°S 60.05°W	368	1980[a],1893[a]	2	Pyroclastic cone(s)
8	Bristol Island	South Sandwich Islands	59.017°S 26.533°W	1100	24.04.2016—19.07.2016 1956, 1950, 1936–1937, 1935, 1823	7	Stratovolcano

Table 1. continuation

No.	Name	Location	Coordinates	Elevation	Eruptions	Number	Type
9	Candlemas Island	South Sandwich Islands	57.08°S 26.67°W	550	1911, 1823	2	Stratovolcano
10	**Montagu Island**	South Sandwich Islands	58.445°S 26.374°W	1370	**2001–2007**	7	Shield
11	**Saunders (Michael)**	South Sandwich Islands	57.8°S 26.483°W	843	**28.08.2015–8.10.2015** **2012, 2010, 2008, 2005–2006, 2003, 2002, 2000–2001, 1997–1998, 1995–1996**	14	Stratovolcano
12	Southern Thule	South Sandwich Islands	59.442°S 27.225°W	1075	1975	1	Stratovolcano (es)
13	**Zavodovski**	South Sandwich Islands	56.3°S 27.57°W	551	**30.03.2016–16.05.2016** 1819	2	Stratovolcano
14	Antuco	Chile	37.406°S 71.349°W	2979	1869, 1863, 1861, 1852–1953, 1845, 1828, 1820–1821, 1806, 1752, 1750	12	Stratovolcano
15	Arenales	Chile	47.2°S 73.48°W	3437	1979	1	Stratovolcano
16	Calbuco	Chile	41.33°S 72.618°W	1974	**22.04.2015–26.05.2015** 1972, 1961, 1945, 1932, 1929, 1917, 1911–1912, 1909, 1907, 1906, 1894–1895, 1893–1894, 1872	17	Stratovolcano
17	Callagui	Chile	37.92°S 71.45°W	3164	1980, 1751	2	Stratovolcano
18	Carrán-Los Venados	Chile	40.35°S 72.07°W	1114	1979, 1955, 1907–1908	4	Pyroclastic cone(s)

Table 1. continuation

No.	Name	Country	Coordinates	Elevation	Eruption years	Count	Type
19	Cerro Hudson	Chile	45.9°S 72.97°W	1905	**2011**, 1991, 1971, 1891, 1740	5	Stratovolcano
20	Chaitén	Chile	42.833°S 72.646°W	1122	**2008–2011**	4	Caldera
21	Copahue	Chile/Argentina	37.856°S 71.183°W	2953	**since 4.06.2017 (ongoing) 18.09.2015–30.12.2016** 2014, 2012–2013, 2000, 1995, 1994, 1992–1993, 1961, 1960, 1944, 1937, 1867, 1750	17	Stratovolcano
22	Descabezado Grande	Chile	35.58°S 70.75°W	3953	1932–1933	2	Stratovolcano (es)
23	Fueguino	Chile	54.97°S 70.262°W	157	1820	1	Lava dome(s)
24	Guallatiri	Chile	18.42°S 69.092°W	6071	1960, 1959, 1913, 1825	4	Stratovolcano
25	Huequi	Chile	42.377°S 72.578°W	1318	1920, 1906–1907, 1900, 1896, 1893, 1890	7	Lava dome(s)
26	Huanquihue Group	Argentina	39.887°S 71.58°W	2189	1750	1	Stratovolcano (es)
27	Irruputuncu	Chile-Bolivia	20.73°S 68.55°W	5163	1995	1	Stratovolcano

Table 1. continuation

#	Name	Country	Coordinates	Elevation	Eruption years	Count	Type
28	Isluga	Chile	19.15°S 68.83°W	5550	1913, 1885, 1878, 1877, 1869, 1868, 1863	7	Stratovolcano
29	Láscar	Chile	23.37°S 67.73°W	5592	**Since 30.10.2015 (ongoing)** **2013, 2006–2007, 2005, 2000**, 1996, 1994–1995, 1993–1994, 1991–1992, 1990, 1987, 1986, 1984–1985, 1969, 1959–1968, 1954, 1951–1952, 1940, 1933, 1902, 1898–1900, 1883–1885, 1875, 1858, 1854, 1848	44	Stratovolcano
30	Lautaro	Chile	49.02°S 73.55°W	3607	1979, 1978, 1972, 1961, 1959–1960, 1945, 1933, 1876	9	Stratovolcano
31	**Llaima**	Chile	38.692°S 71.729°W	3125	**2008–2009, 2007, 2003, 2002**, 1998, 1997, 1995, 1994, 1992, 1990, 1984, 1979, 1971, 1964, 1960, 1955–1957, 1949, 1946, 1945, 1944, 1942, 1941, 1938, 1937, 1932–1933, 1930, 1929, 1927, 1922, 1917, 1914, 1912, 1907–1908, 1903, 1895–1896, 1892, 1893–1894, 1889, 1887, 1883, 1877, 1875, 1872, 1869, 1866, 1864, 1862, 1852, 1822, 1759, 1751–1752, 1642	60	Stratovolcano
32	Llullaillaco	Chile-Argentina	24.72°S 68.53°W	6739	1877, 1868, 1854	3	Stratovolcano
33	Longuimay	Chile	38.379°S 71.586°W	2832	1988–1990, 1933, 1887–1890, 1853	9	Stratovolcano
34	Maipo	Chile	34.164°S 69.832°W	5323	1912, 1905, 1829, 1826	4	Caldera
35	Mentolat	Chile	44.7°S 73.08°W	1660	1710	1	Stratovolcano
36	Michinmahuida	Chile	42.799°S 72.445°W	2452	1835, 1934, 1742	3	Stratovolcano

Table 1. continuation

No.	Name	Country	Coordinates	Elevation	Eruption years	No.	Type
37	Mocho-Choshuenco	Chile	39.927°S 72.027°W	2422	1937, 1864	2	Stratovolcano (es)
38	Nevados de Chillán	Chile	36.863°S 71.377°W	4750	**Since 08.01.2016 (ongoing)** **2003**, 1973–1986, 1946–1947, 1935, 1934, 1928–1929, 1927, 1914, 1907, 1906, 1898, 1893, 1891, 1877, 1872, 1864, 1861–1863, 1860, 1752, 1749–1751, 1650	41	Stratovolcano
39	Olca-Paruma	Chile-Bolivia	20.939°S 68.413°W	5705	1865	1	Stratovolcano (es)
40	Osorno	Chile	41.105°S 72.496°W	2659	1869, 1855, 1851, 1837, 1834–1835, 1790–1791, 1765, 1719, 1644, 1640, 1575	13	Stratovolcano
41	Planchón-Peteroa	Chile	35.223°S 70.568°W	3977	**2011**, **2010**, 1998, 1991, 1962, 1960, 1959, 1938, 1937, 1889, 1878, 1860, 1837, 1835, 1762, 1751, 1660	17	Stratovolcano (es)
42	Puntiagudo-Cordón Cenizos	Chile	40.969°S 72.264°W	2493	1850	1	Stratovolcano
43	Putana	Chile	22.557°S 67.853°W	5884	1810	1	Stratovolcano
44	**Puyehue-Cordón Caulle**	Chile	40.59°S 72.117°W	2236	**2011–2012**, 1990, 1960, 1934, 1929, 1921–1922, 1919–1920, 1914, 1905, 1893, 1759	14	Stratovolcano
45	Quetrupillan	Chile	39.5°S 71.7°W	2360	1872	1	Stratovolcano
46	Reclus	Chile	50.964°S 73.585°W	1000	1908, 1879, 1869, 1830	4	Pyroclastic cone
47	**Sabancaya**	Peru	15.787°S 71.857°W	5960	**Since 06.11.2016 (ongoing)** **2015**, **2003**, 2000, 1990–1998, 1988, 1986, 1794, 1750	18	Stratovolcano (es)

Table 1. continuation

48	San José	Chile	33.789°S 69.895°W	6070	1960, 1959, 1985–1989, 1889–1890, 1881, 1838, 1822–1838	28	Stratovolcano(es)
49	San Pedro-San Pablo	Chile	21.888°S 68.391°W	6142	1960, 1938, 1911, 1901, 1891, 1877	6	Stratovolcano(es)
50	Tinguiririca	Chile	34.814°S 70.352°W	4280	1917	1	Stratovolcano
51	Tromen	Argentina	37.144°S 70.033°W	4114	1822, 1751	2	Stratovolcano(es)
52	Tupungatito	Chile-Argentina	33.425°S 69.797°W	5660	1987, 1986, 1980, 1968, 1964, 1961, 1960, 1959, 1958, 1946–1947, 1925, 1907, 1901, 1897, 1889–1890, 1861, 1829	19	Stratovolcano
53	Viedma	Argentina	49.358°S 73.28°W	1500	1988	1	Subglacial
54	**Ubinas**	Peru	16.355°S 70.903°W	5672	**13.09.2016—02.03.2017** 2013–2016, 2006–2009, 1969, 1956, 1951, 1937, 1907, 1906, 1869, 1867, 1865, 1862, 1830, 1784, 1677, 1667, 1662, 1550	24	Stratovolcano
55	**Villarica**	Chile	39.42°S 71.93°W	2847	**Since 2.12.2014 (ongoing)** 2013, 2012, 2009–2012, 2009, 2008, 2004–2007, 2003– 2004, 1998–2002, 1996–1997, 1995, 1994, 1992, 1991, 1984–1985, 1983, 1980, 1977, 1971–1972, 1964, 1963, 1961, 1958–1959, 1956, 1948–1949, 1948, 1947, 1938– 1939, 1935–1936, 1933, 1929, 1927–1928, 1922, 1920, 1915, 1909–1910, 1908, 1907, 1906, 1904, 19024, 1897– 1898, 1893–1894, 18904, 1883, 1880, 1879, 1877, 1875, 1874, 1871[4], 1869, 1864, 1859–1860, 1853, 1850[4] 1841, 1837, 1836, 1832, 1826[4], 1822, 1815–1818, 1806, 1798[4] 1790–1801, 1787, 1780, 1777, 1771[d], 1767[d] 1761[d], 1759, 1751, 1745, 1742, 1737, 1730, 1721[d] 1716, 1715[d] 1709[d] 1708[d] 1705[d] 1688, 1682[d] 1675[d] 1672[d] 1669[d] 1657, 1647, 1645[d] 1642[d] 1638[d] 1632[d] 1625[d] 1617[d] 1612[d] 1610[d], 1604[d] 1600[d] 1594, 1584[d] 1582[d] 1579[d] 1564[d],1562, 1558	142	Stratovolcano

Table 1. continuation

No.	Name	Country	Coordinates	m a.s.l.	Eruption years	No.	Type
56	Okataina	New Zealand	38.12°S 176.5°E	1111	1981, 1978, 1973, 1951,1926, 1924, 1918, 1917, 1915, 1914, 1913, 1912, 1910, 1908, 1906, 1905, 1900, 1896, 1886	19	Lava dome(s)
57	**Ruapehu**	New Zealand	39.28°S 175.57°E	2797	**2007, 2006**, 1997, 1996, 1995, 1992, 1991, 1990, 1988–1989, 1987, 1986, 1985, 1984, 1981–1982, 1980, 1977–1979, 1976, 1975, 1973–1974, 1972–1973, 1971, 1970, 1969, 1968, 1967, 1966, 1959, 1956, 1952, 1951, 1950, 1948, 1946–1947, 1945, 1944, 1942, 1940, 1936, 1934, 1925, 1921, 1918, 1906, 1903, 1895, 1889, 1861	54	Stratovolcano
58	**Raoul Island**	New Zealand	29.27°S 177.92°W	516	**2006**, 1964–1965, 1886, 1870, 1814	6	Stratovolcano
59	Taranaki	New Zealand	39.3°S 174.07°E	2518	1854	1	Stratovolcano
60	Tongariro	New Zealand	39.157°S 175.632°E	1978	**2012**, 1977, 1976, 1975, 1972–1974, 1969, 1968, 1962, 1959, 1958, 1956, 1954, 1952–1953, 1951, 1950, 1949, 1948, 1940, 1939, 1937, 1934–1935, 1931, 1928, 1926, 1925, 1924, 1917, 1914, 1913, 1910, 1909, 1907, 1906, 1905, 1904, 1898, 1897, 1896, 1892, 1886, 1884–1885, 1883, 1881, 1878, 1870, 1869, 1864–1865, 1863, 1862, 1859, 1857, 1855, 1844–1845, 1841, 1839	62	Stratovolcano (es)
61	**White Island**	New Zealand	37.52°S 177.18°E	321	13.09.2016, 27.04.2016, **2012–2013, 2001, 2000, 1998–1999, 1995**, 1986–1994, 1983–1984, 1976–1982, 1974, 1971, 1970, 1969, 1968–1969, 1966–1967, 1962, 1959, 1958, 1957, 1955, 1947, 1933, 1930, 1928, 1926, 1924, 1922, 1909, 1886, 1885, 1836, 1826	49	Stratovolcano (es)

Abbreviation: m a.s.l - metres above sea level; N – North; E – East

[a]uncertain, [b]tephrochronology, [c]lichenometry, [d]varve cou

Particular attention was placed on air mass inflow trajectories from September 2015 to August 2017. This choice of period was dictated by the project implemented in the years 2015–2020, "Identification and determination of concentrations and translocation levels of atmospheric pollutants in water bodies as an indicator of the adaptive capacity of the Antarctic". The objective of that research is to gain an in-depth understanding of the chemical composition of water samples from watercourses, lakes and glacial outflows, and samples of soil and coastal seawater sediment from the western shore of Admiralty Bay, and to identify how that composition varies over time and identify pathways of potential contaminants (Szopińska et al. 2018).

The air masses' trajectories were compared with volcanic activity in the Southern Hemisphere. The data of volcanic activity is available in the Global Volcanism Program database (www.volcano.si.edu) for the research period 2015–2017 and historical times. However, for the purposes of this work particular volcano cards were analysed to complete the data in Table 1. The need to take into account historical data was dictated by the fact that any volcanic compounds reaching the South Shetland Islands could have accumulated in glacial ice and then been released into the environment during melt periods.

Directions of long-range air mass transport to the South Shetland Islands in September 2015 – August 2017

In the study period September 2015 to August 2017, the air masses flowing into the South Shetland Islands were most often from the Antarctic area (latitudes above 60°S, Table 2). However, the direction of incoming air masses was not always compatible with circumpolar air circulation. The air masses forming over the Southern Ocean were observed on all days of researched period, and on 355 days air masses were formed over the Antarctic continent. The total number of days with LRAT observed in the South Shetland Islands during the 24 researched months was 319, which is 44% of the total number of analysed days. The LRAT

occurred most often from May to October, in the autumn and winter seasons (Fig. 2), and the most frequent LRAT in SSI was observed in July 2016 (23 days). Taking into account directions of incoming air masses during the analysed 731 days, the air masses came 226 times from South America, 29 times from the South Sandwich Islands, 92 times from New Zealand, 39 times from the south-west coast of Australia (Table 2, Fig. 3) and once from the region of Madagascar (19.09.2016).

The most frequent source area of LRAT in the SSI is South America (Table 2, Fig. 3). In the researched period it was mainly in the winter months that air masses came from SA, with the highest frequency in July and August 2016 and August 2017 (Fig. 3). As mentioned above, most of the active volcanoes in South America are located in the west of the continent. Air masses originating from the south-west coast of South America flowed in over the South Shetland Islands with varying frequency over the study period (Fig. 3), with air masses sometimes having started in the Patagonian volcanic region at the 20°S latitude range (Table 2 – highlighted data, Fig. 4). During the analysed period, the mentioned air masses originated from the volcanic region on selected days of October 2015, May, July, August and October 2016, and April, May, June and August 2017 (Table 2). In this area some of the most active volcanoes are found, e.g. Copahue, Nevados de Chillán and Villarica. The Copahue volcano, located in the Patagonian Andes (37.9°S, 71.2°W) has been active every year since 2012, with continuous activity since June 4th 2017 (Table 1, Fig. 3). Similarly constant activity has characterised the volcano Nevados de Chillán (36.9°S, 71.4°W) since January 1st 2016, and the volcano Villarica (39.4°S, 71.9°W) since December 2nd 2014. This last volcano has been active for a total of 142 years since 1558. These volcanoes being active during the inflow of air masses from Patagonia towards Antarctica (Fig. 3) was a source of volcanic steam and ash entering the atmosphere, e.g. in May 2016 and between February 2017 and November 2017 (Global Volcanism Program, www.volcano.si.edu). Moreover, in the researched period another three volcanos were active, those being located in the central part of Andes Mountains: Láscar, Sabancaya and Ubinas (Table 1, Fig. 1). During the researched period air masses came from this area once, on

Table 2. Air mass source areas for the South Shetland Islands September 2015 – August 2017 (prepared based on 10-day back trajectories of air masses at heights 500 m, 1,000 m and 2,000 m, calculated with the HySPLIT model based on Global Data Assimilation System meteorological data). Dates with different air mass directions marked in bold, underlined dates - with air masses coming from volcanic area

		A	O	SA	SI	NZ	AU
2015	IX 2015	2, 3, 4, 5, 6, **7**, 8, **9**, **11**, 12, 13, 14, **15**, 16, 17, **18**, 20, 21, 22, 24, 25, 26, 28, 29, **30**	**1**, 2, 3, 4, 5, 6, **7**, 8, **9**, 10, 11, 12, 13, 14, **15**, 16, 17, **18**, 19, 20, 21, 22, 23, 24, 25, 26, 27, 28, 29, **30**	7, 9, 15, 18, 30	18	11	1
	X 2015	**1**, 2, **6**, 8, **9**, 10, 13, 14, 15, **16**, **18**, **19**, 20, 21, 22, 24, 26, **27**, 28, **29**, **31**	**1**, 2, **3**, **4**, **5**, **6**, 7, 8, **9**, 10, **11**, 12, 13, 14, 15, **16**, **17**, **18**, **19**, 20, 21, 22, 23, 24, **25**, 26, **27**, 28, **29**, 30, 31	3, 4, <u>5</u>, <u>6</u>, 19, 27		1, 7, **9**, **11**, 16, 17, 18, **19**, 27, **29**, 31	7, 9, **11**, 16, 17, 18, 25, 31
	XI 2015	1, **4**, 5, 7, 8, 11, 12, 14, 15, 16, 17, **19**, **21**, 23, 24, 25	1, 2, **3**, **4**, 5, 6, 7, 8, 9, **10**, 11, 12, **13**, 14, 15, 16, 17, **18**, **19**, **20**, **21**, 22, 23, 24, 25, 26, 27, 28, **29**, 30	4, 13, **18**, **19**, **20**, **21**		3, 29, 30	10, 30
	XII 2015	1, 2, **3**, 4, 5, **7**, **8**, **9**, 10, **12**, 13, **14**, **17**, 18, **19**, **24**, 27, 28, **29**, 30, 31	1, 2, 3, 4, 5, 6, **7**, **8**, **9**, 10, 11, 12, 13, **14**, **15**, **16**, **17**, 18, **19**, 20, 21, **22**, 23, **24**, **25**, **26**, 27, 28, **29**, 30, 31	3, 7, **14**, **15**, **16**, **17**, 19, **22**, 24, **25**, **26**, 29, 30	12, 14, 15,	8, 9, 19	
2016	I 2016	1, 5, 8, **9**, 11, 12, 15, 16, 17, 18, 19, 20, 22, 23, 24, 28, 30, **31**	1, **2**, **3**, 4, 5, 6, 7, 8, **9**, 10, 11, 12, 13, 14, 15, 16, 17, 18, 19, 20, 21, 22, 23, 24, **25**, 26, 27, 28, **29**, 30, 31	**2**, **3**, **9**, 25		2, 29, 31	29
	II 2016	2, 8, 9, **10**, 12, 13, **14**, 15, 19, **24**, **25**, 26,	1, 2, **3**, **4**, 5, **6**, 7, 8, 9, **10**, **11**, 12, 13, **14**, **15**, 16, **17**, 18, 19, **20**, **21**, 22, 23, **24**, **25**, 26, 27, **28**, 29	4, **14**, **17**, **20**, **21**, **24**, **25**, **28**,		3, 10, 11, 12, 17, 20	6
	III 2016	**3**, 10, 13, 14, 17, 19, **23**, **27**, **30**, **31**	**1**, 2, **3**, **4**, 5, 6, 7, 8, 9, 10, **11**, **12**, 13, 14, 15, 16, 17, 18, 19, 20, **21**, 22, **23**, 24, 25, 26, **27**, 28, 29, **30**, **31**	4, **11**, **23**, 27, **30**, 31		3, 21	1
	IV 2016	1, 2, 3, 4, 5, 7, 8, 9, 11, 12, 13, 15, 17, 18, 19, 20, 21, **22**, 23, **24**, 28	1, 2, 3, 4, 5, **6**, 7, 8, 9, 10, 11, 12, 13, **14**, 15, **16**, 17, 18, 19, 20, 21, **22**, 23, **24**, 25, **26**, **27**, 28, 29, 30	**6**, **14**, **22**, **24**, 27		16, 26	

Table 2. continuation

2016	Month					
2016	V 2016	**1**, 2, **3**, **4**, 5, 6, **7**, 11, 17, 24, 25, 31	**1**, 2, **3**, **4**, 5, 6, **7**, 8, 9, 10, 11, **12**, **13**, 14, **15**, 16, 17, **18**, **19**, **20**, 21, **22**, 23, 24, 25, **26**, **27**, **28**, **29**, **30**, 31	3, 4, 7, **18**, **19**, 20, <u>26</u>, 27, 28, <u>29</u>, <u>30</u>		**1, 7, 12, 13, 15, 18, 22**	**7**
	VI 2016	1, 3, 4, 5, **6**, 7, **14**, 22, **23**, 27, 28, **29**, 30	1, 2, 3, 4, 5, **6**, 7, **8**, 9, 10, 11, **12**, 13, **14**, 15, 16, **17**, **18**, **19**, 20, **21**, 22, **23**, **24**, **25**, 26, 27, 28, **29**, 30	14, 18, 24, 25, 29		**6, 8, 12, 17, 19, 21, 23**	**19**
	VII 2016	1, **2**, 4, 5, 6, **8**, **9**, **10**, **11**, **12**, **13**, 22, **23**, **24**, 25, 26	1, **2**, 3, 4, 5, 6, **7**, **8**, **9**, **10**, **11**, **12**, **13**, **14**, **15**, **16**, **17**, **18**, **19**, **20**, **21**, **22**, **23**, **24**, 25, 26, 27, **28**, **29**, **30**, **31**	7, 8, 9, 10, 12, 13, 14, 17, 18, 19, 21, 22, 23, 24, 28, <u>29</u>, <u>30</u>, 31	7, 8, 9, 10, 11, 13	2, 16, 17, 19, 21	**15, 20**
	VIII 2016	2, 3, **5**, 9, **10**, **11**, 12, **13**, **14**, **15**, **16**, **17**, 18, 21, 22, **23**, **24**, **25**, **26**, 27, 28	1, 2, 3, **4**, 5, **6**, **7**, **8**, 9, **10**, **11**, 12, **13**, **14**, 15, **16**, **17**, 18, **19**, 20, 21, 22, **23**, **24**, **25**, **26**, 27, 28, **29**, **30**, **31**	4, 6, 7, 8, <u>10</u>, 11, 13, 14, 15, 17, 19, 23, 24, 25, 26, <u>29</u>, <u>30</u>, <u>31</u>	14, 15, 16, 17	4, 6, 7, 29	6, 30
	IX 2016	2, 6, 9, 17, 26, 28	**1**, 2, **3**, **4**, 5, 6, **7**, **8**, 9, 10, **11**, 12, 13, **14**, **15**, 16, 17, **18**, **19**, **20**, 21, **22**, 23, 24, **25**, 26, **27**, 28, 29, 30	1, 4, 7, 8, 14, 15, 20, 21, 22, 27		3, 19	3, 11, 18, 24, 25
	X 2016	5, **8**, **12**, **16**, 17, **18**, 23, 26, 27, **30**	1, **2**, **3**, **4**, 5, 6, **7**, **8**, 9, **10**, **11**, **12**, **13**, **14**, **15**, 16, 17, **18**, 19, 20, **21**, **22**, 23, 24, **25**, 26, 27, 28, **29**, 30, 31	<u>3</u>, 4, 7, 8, 11, 12, 13, 14, 15, 16, **29**, **30**, 31	10	2, 18, 21, 22, 25	2, 18, 30
	XI 2016	**1**, **3**, 4, **5**, 7, **8**, 13, 14, 15, **16**, 17, 18, 22, 23, 25, 26	**1**, 2, 3, 4, **5**, **6**, 7, **8**, **9**, **10**, 11, **12**, 13, 14, 15, **16**, 17, 18, **19**, **20**, 21, 22, 23, 24, 25, 26, 27, **28**, 29, 30	1, 3, 5, 8, 9, 10, 12, **16**, 19, 20		28	6, 28
	XII 2016	3, 7, 13, 23, 27, 28,	1, **2**, 3, 4, **5**, **6**, 7, 8, 9, 10, 11, 12, 13, 14, **15**, 16, **17**, **18**, **19**, **20**, **21**, **22**, 23, 24, **25**, **26**, 27, 28, 29, 30, 31	2, 5, 15, 17, 18, 19, 20, 21, 22, 25, 26		6, 15, 20, 22	6

Table 2. continuation

	Month						
2017	I 2017	4, 5, 6, **7**, **8**, **10**, 14, **15**, 25, 26, 29, 30	1, 2, 3, 4, 5, 6, **7**, **8**, **9**, **10**, **11**, **12**, **13**, 14, **15**, 16, **17**, **18**, **19**, 20, **21**, 22, 23, 24, 25, 26, **27**, 28, 29, 30, 31	**7**, **8**, **9**, **10**, **11**, **17**, **19**, **21**, **27**	**12, 13, 15, 18**	**12, 18, 21**	
	II 2017	2, 3, 4, 5, 6, 7, **8**, 17, **19**, 20, 21, **23**, **24**, 25	1, 2, 3, 4, 5, 6, **8**, **9**, **10**, **11**, **12**, **13**, **14**, 15, **16**, 17, 18, **19**, 20, 21, **22**, **23**, **24**, 25, **26**, 27, 28	**8, 9, 10, 14, 16, 19, 23, 26**		**9, 11, 12, 13, 22, 24**	**9**
	III 2017	1, 2, **3**, 4, 5, 6, 7, 8, 9, 15, 17, 26	1, 2, **3**, 4, 5, 6, 7, 8, 9, 10, 11, 12, **13**, **14**, 15, 16, 17, 18, 19, 20, **21**, **22**, 23, 24, 25, 26, 27, **28**, 29, 30, 31	**3, 13, 14, 21**		22, 28	28
	IV 2017	3, 6, 7, 11, **21**, 22, **23**, 24, 25, 26, 27, 28, 29, 30	1, 2, 3, **4**, 5, 6, 7, 8, 9, 10, 11, 12, 13, 14, **15**, **16**, **17**, **18**, **19**, **20**, **21**, 22, **23**, 24, 25, 26, 27, 28, 29, 30	**4**, <u>20</u>, 21, 23		4, 15, 16, 17	15, 18, 19
	V 2017	4, **5**, **6**, 7, 9, 17, **25**, 26, 27, 28, 29, 30	**1, 2, 3**, 4, **5, 6**, 7, **8, 9**, 10, 11, **12, 13**, 14, **15, 16**, 17, **18, 19**, 20, **21, 22, 23**, 24, **25**, 26, 27, 28, 29, 30, 31	1, 2, 3, 6, <u>15</u>, 16, 18, 19, 21, 22, 23, 25		5, 8, 12, 13	18
	VI 2017	**1, 2**, 16, **18**, 19, 21, 22, 23, 24, 25, 27, 29, 30	**1, 2, 3, 4, 5, 6**, 7, 8, **9, 10, 11, 12, 13, 14, 15**, 16, 17, **18**, 19, 20, 21, 22, 23, 24, 25, 26, 27, 28, 29, 30	2, 3, 4, 5, <u>6</u>, 7, 9, 10, 11, 12, 13, 14, 15	10, 12, 15	1, 18	
	VII 2017	8, **9**, 10, 11, 12, 16, 17, 18, 19, 20, 21, **22**, 23, **24**, **25**, 28, 30	1, **2**, 3, 4, 5, 6, **7**, 8, **9**, 10, 11, 12, **13**, **14**, **15**, 16, 17, 18, 19, 20, 21, **22**, 23, **24**, **25**, **26**, **27**, 28, **29**, 30, **31**	2, 5, 6, 7, 9, 13, 14, 15, 26, 27, 29	22, 24, 25, 26	31	9, 14
	VIII 2017	1, 2, **3**, **5**, 6, 7, **11**, **12**, 19, **21**, **24**, **25**, **26**, 27, 28, 29, 30	1, 2, **3**, 4, **5**, 6, 7, 8, **9**, **10**, **11**, **12**, 13, **14**, **15**, **16**, 17, **18**, 19, **20**, 21, **22**, **23**, **24**, **25**, **26**, 27, 28, 29, 30, 31	9, <u>10</u>, <u>11</u>, 12, 14, <u>15</u>, <u>16</u>, 17, 18, 20, 21, 22, <u>23</u>, <u>24</u>, 25, 26	16, 17, 18	3, 5, 15, 16	
	Total No.	355	731	226	29	92	39
	%	49	100	31	4	13	5

Abbreviation: A – Antarctica, SA – South America, SI – South Sandwich Islands, NZ – New Zealand, AU – Australia

May 15th 2017. Similarly, the activity of the Bristol volcano on the South Sandwich Islands coincided with the inflow of air masses towards the South Shetland Islands (Fig. 3).

The other presented source areas of air masses incoming to SSI are less frequent (Table 2, Fig. 3). It should be noted that air masses coming from the Eastern Hemisphere usually have two sourcing areas – both New Zealand and Australia – but the former area was the more frequent source of air masses incoming to SSI, at 92 days, compared to 39 days for the latter. These air masses occur less frequently than air masses originating over South

America (Fig. 3). Air masses originating over New Zealand and Australia occurred most frequently in October 2015, and additionally in the case of New Zealand in February, May, June 2016, and in February 2017. However, during the White Island volcano eruptions observed on April 27th and September 13th 2016, air masses incoming to SSI have another source area.

It is also worth noticing that air masses originating over South America and South Sandwich Islands reached SSI in 1–3 days (Figs 4A and B), but the time of transport of air masses forming over
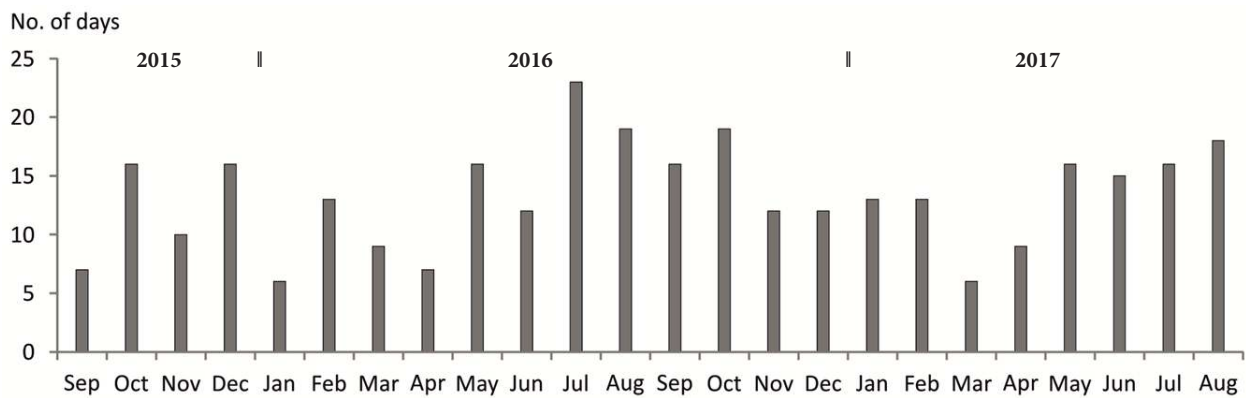
Fig. 2. Total number of days with LRAT in the South Shetland Islands in the particular months during researched period Sep 1st 2015 – Aug 31st 2017, (prepared base on 10-day back trajectories of air masses at heights 500 m, 1,000 m and 2,000 m calculated with the Hy-SPLIT model based on Global Data Assimilation System meteorological data).
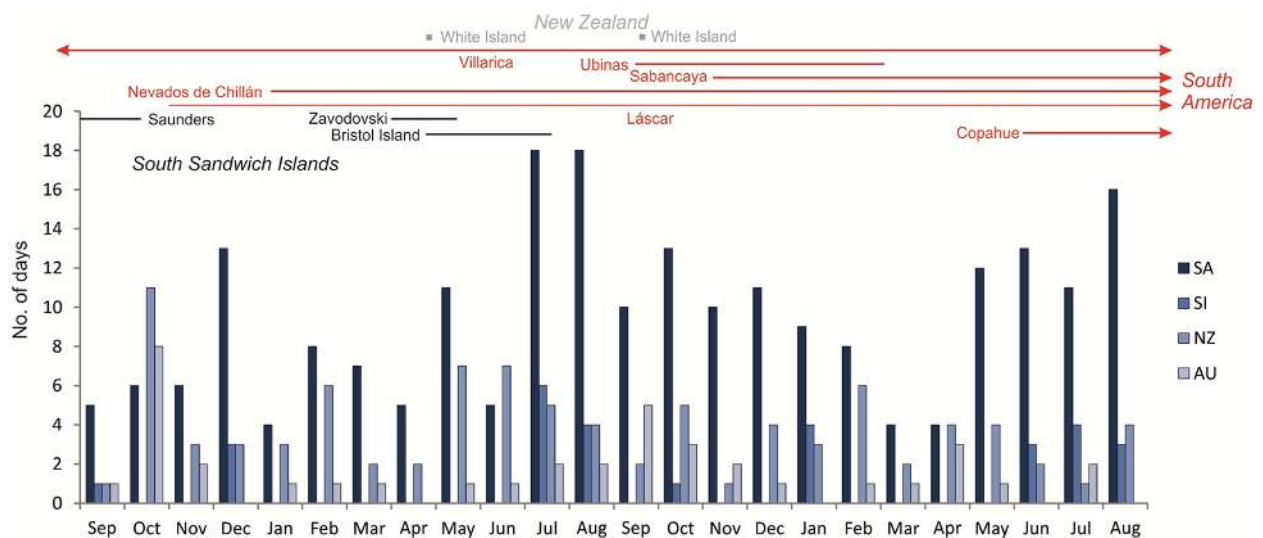
Fig. 3. Total number of days with air masses incoming from SA – South America, SI – South Sandwich Islands, NZ – New Zealand, AU – Australia in individual months during researched period Sep 1st 2015 – Aug 31st 2017 compared with volcanoes' activity (prepared based on 10-day back trajectories of air masses at heights 500 m, 1,000 m and 2,000 m calculated with the HySPLIT model based on Global Data Assimilation System meteorological data, Global Volcanism Program, www.volcano.si.edu).
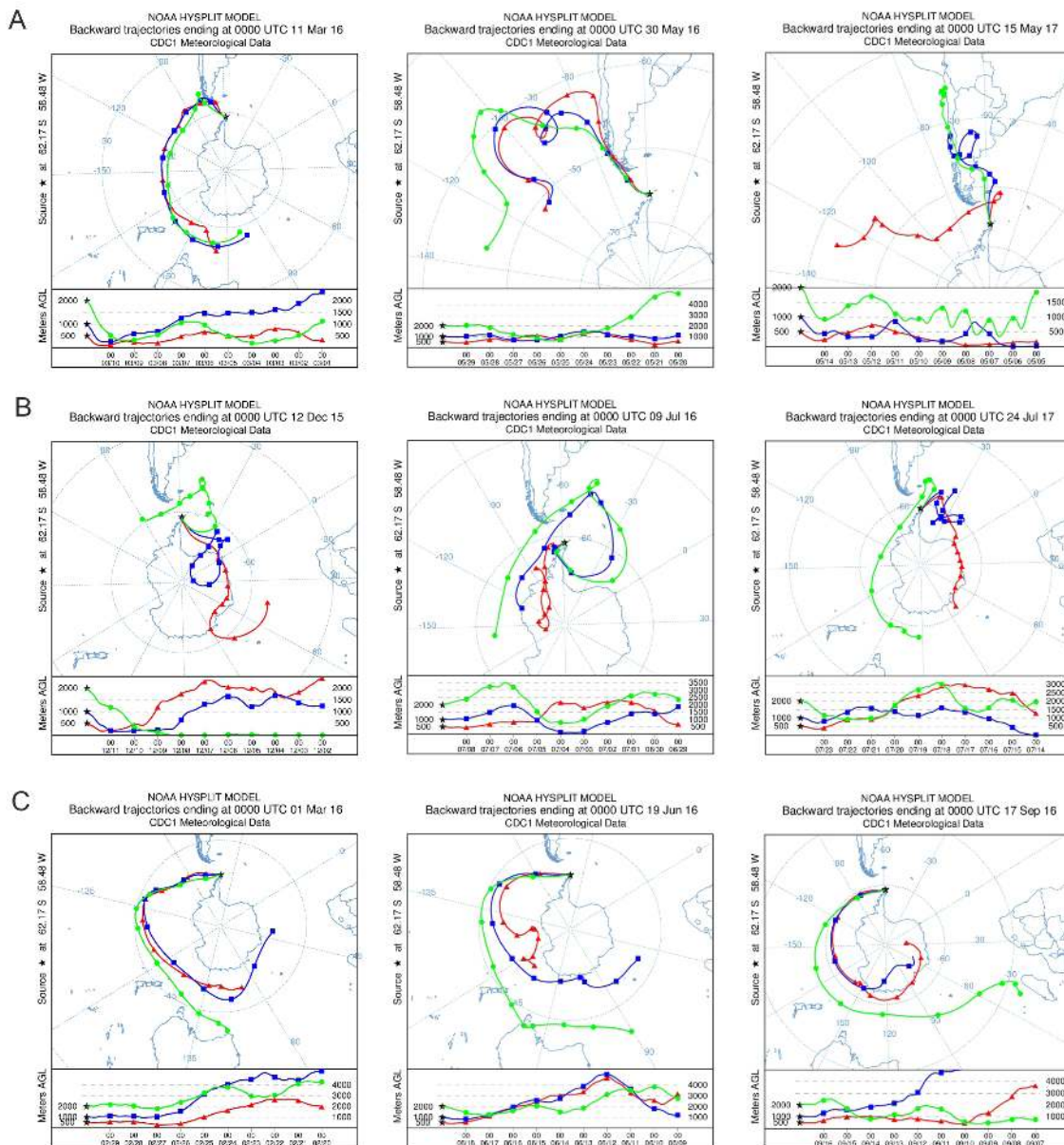
Fig. 4. Selected 10-day back trajectories of air masses at heights 500 m, 1,000 m and 2,000 m for September 2015 – August 2017: A – air masses originating from South America, B – air masses originating from South Shetland Islands, C – air masses originating from New Zealand and Australia (calculated with the HySPLIT model based on Global Data Assimilation System meteorological data.

Table 3. Correlations and statistical significance between monthly occurrence of LRAT and selected directions of air-masses and SAM and El Niño3.4 indices during the period between September 2015 and August 2017. p-values are indicated in parentheses. Bolded values indicate statistically significant correlations at 95% confidence (SAM indices obtained from https://legacy.bas.ac.uk/met/gjma/sam.html; El Niño3.4 indices obtained from https://www.esrl.noaa.gov/psd/gcos_wgsp/Timeseries/Nino34/).

	ENSO	SAM	SA	NZ	LRAT
ENSO	1.00				
SAM	**0.46 (0.025)**	1.00			
SA	**–0.46 (0.025)**	–0.30 (0.154)	1.00		
NZ	0.09 (0.664)	–0.11 (0.607)	0.01 (0.955)	1.00	
LRAT	**–0.41 (0.049)**	–0.26 (0.230)	**0.88 (0.000)**	0.36 (0.086)	1.00

New Zealand and Australia was longer, and it was usually 7–10 days (Fig. 4C).

Correlation between the number of days with LRAT in the SSI and SAM (the South Annual Mode) and ENSO (El Niño3.4 indices) show a statistically significant negative correlation (in the 95% confidence range) between the number of days with LRAT and the ENSO indices. This correlation depends basically on negative correlation between advection of air masses from the South American direction and ENSO.

Discussion

Air mass advection into the South Shetland Islands

Many authors have pointed out that some contaminants occurring in Antarctica could be related to LRAT (*inter alia*, Lee et al. 2004, 2007; Klánová et al. 2008; Chambers et al. 2014; McConnel et al. 2014), but there is still little knowledge about the frequency of air masses incoming from lower latitudes to the Antarctic Peninsula. The 10-day back trajectories for the period September 2015 to August 2017 show that long-range transport by air masses to the South Shetland Islands occurs relatively often (44% of researched days) and the most frequent source area is South America (31% of researched days). According to Kejna (1993) the advection of air masses to King George Island is shaped mostly by cyclonic circulation (69% during the period 1986–1989). Moreover, the author concluded that the most frequent directions of air masses incoming to Arctowski Station (King George Island, SSI) are from a westerly or north-westerly direction. Both the cyclonic and anticyclonic types of air masses moving from these directions in the researched period constitute in total 34.9% of air masses (Kejna 1993). It can therefore be concluded that the frequencies of westerly and north-westerly directions of air masses described by Kejna (1993) for the years 1986–1989 are similar to the frequency of air masses incoming from South America in the years 2015–2017 (31%). Our study indicated that air masses originating over SA could also come

from the north-east, east and south-east, but that the westerly and north-westerly directions are the most frequent. The latest results of atmospheric patterns over Antarctic Peninsula (Gonzalez et al. 2018) including the period 1979–2016 show the dominance of five patterns of cyclonic circulation over the Antarctic Peninsula. Most are related to the zonal moving of lows, but some of them support meridional paths from the north, e.g. Low over the Drake Passage (LDP), Ridge over the Antarctic Peninsula (RAP). In two works related to synoptic conditions in this area (Kejna 1993; Gonzalez et al. 2018) both authors located the centres of lows in the high latitudes, to the north-west, north or south-west of the Antarctic Peninsula. This location supports the movement of air masses from the direction of SA. Moreover, Gonzalez et al. (2018) analysed the relation between SAM (the Southern Annual Mode) and ENSO events (El Niño 3.4 index) and the occurrence of particular synoptic patterns, and concluded that SAM supports the zonal path of lows. Related to their results, ENSO events have a lesser impact on the synoptic situation over the Antarctic Peninsula. However, the negative correlation between ENSO and advection of air masses to SSI from the direction of South America in the researched period show that temporal changes of ENSO may have influenced the frequency of LRAT (Table 3).

Volcanic activity as a source of contaminants delivered by long range atmospheric transport into the South Shetland Islands

Direct observations of contemporary volcanic eruptions in South America indicate that volcanic ashes can travel in the atmosphere from the Patagonia region to the eastern edge of South America in just two days (Durant et al. 2012). The aforementioned authors have recorded volcanic ashes with a diameter of 32 μm ± 5 μm being transported between 95 and 530 km from the volcano during the period 3–7 May 2008, and calculated that 0.2–0.4 Tg of airborne ash was suspended in the atmosphere. It is relatively easy to identify the movement of volcanic ash because it is clearly visible in satellite images. Howev-

er, volcanic eruptions are also a source of volatile and medium volatile compounds, including PAHs (semi-volatiles) (Fuoco et al. 2012), which can be transported between continents with volcanic ash) (e.g. Ravindra et al. 2008; Kozak et al. 2017). Their movement paths have not thus-far been identifiable using satellite data, but in various parts of the world they are interpreted using air mass trajectories (*inter alia*, Van Drooge et al. 2010; Kozak et al. 2017). It should also be noted that in order for volcanic compounds to reach the South Shetlands, volcanic activity (eruption or dust and gas eruptions) must coincide with air masses moving towards Antarctica (Tables 1 and 2, Fig. 3). If we assume, on the basis of air mass trajectories presented herein and by other authors (Lee et al. 2004, 2007; Chambers et al. 2014; McConnel et al. 2014), that such transport is possible, and we take into account the high activity of volcanoes in the Southern Hemisphere (Table 1), it can be assumed that such events could have occurred in the past. The model of the global distribution of volcanic sulphur (Graf et al. 1997) confirms the possibility of this source of compounds influencing the Antarctic environment. However, analyses of single volcanic events (Table 1) show that particular eruptions may influence the ocean surrounding the Antarctic region, excluding terrestrial areas (Klüser et al. 2013). Therefore, considering the possibility of volcanic compounds being redistributed by marine aerosols (e.g. boron), and the influence of local-Antarctic volcanoes on the atmosphere and ocean (Graf et al. 2010) the question of the paths along which these compounds are transported may constitute the basis for further research.

Another observation of LRAT's influence on temporal changes in air chemistry was conducted by Chambers et al. (2014). Using a combination of back-trajectory analyses and radon content in air masses, the authors identified South America as a fetch region for terrestrially influenced air masses arriving in the Antarctic Peninsula. Air masses originating from this region caused high radon "events" on the peninsula. Moreover, research of soil chemistry conducted on Barton Peninsula shows that volcanic ash originating from Patagonia reached SSI (Lee et al. 2004). Based on the REEs (rare earth elements) Rb, Sr, Ba, Cr, Co, Ni and V in soils, those authors stated that the main source of elements was local volcano eruptions (Deception

Island volcano) and secondary atmospheric dusts sourced from Patagonia. Similar results were obtained in a previous study by the authors of this paper (Szopińska et al. 2018). Boron, which is relatively well represented in water samples (Szopińska et al. 2018) originates from marine aerosols and is a volatile element accompanying volcanic activity (Katalin et al. 2007). It is worth nothing that Rb, Sr, Ba and V, to which Lee et al. (2004) attributed a volcanic origin, was also determined in fresh water samples at the western shore of Admiralty Bay, and the strong correlation of Sr concentration with marine aerosols shows its origin to be from atmospheric transport (Szopińska et al. 2018). The analysis of back trajectories of air masses presented in this work shows the relative high frequency of South America being the fetch region for air masses. On the other hand, a lot of volcanoes were active in the past in this area, and some are still the sources of compounds in the air, e.g. PAHs. The presented results confirm the possibility of LRAT of volcanic compounds (Lee et al. 2004; Chambers et al. 2014), because, in the researched period during the time of high frequency of advection from SA, several volcanoes were active.

The numerous tephra layers found in the lakes on the South Shetland Islands (Björck et al. 1991; Hodgson et al. 1998; Tatur et al. 1999; Lee et al. 2007; Aymerich et al. 2016; Liu et al. 2016) and the South Orcan Islands (Hodgson et al. 1998) are evidence of the influence of volcanic eruptions on the Antarctic environment. The mentioned authors connect the prevailing tephra horizons with Deception Island volcano activity in the Holocene; however, Lee et al. (2007) suggested that the source volcano(es) for about 10% of basic tephra and silicic tephra are not readily identified from nearby volcanic centres. Tephra horizons also show that the Deception Island volcano is a possible source of contaminants of volcanic origin that may accumulate in Antarctica and be transported by LRAT to the highest latitudes. The eruption of this volcano in 1970 caused transport of pyroclastic material and an eruptive column at least 10 km high, from which deposits are recognised more than 100 km to the NE (Pedrazzi et al. 2014). The effects

of two 17th-century eruptions of this volcano were recorded in ice drilled on the James Ross Island (Antarctic Peninsula) (Aristarain and Delmas 1998). Geyer et al. (2017) evaluated the potential impacts of ash from Deception Island assuming several eruption scenarios. According to the presented simulations the aforementioned authors concluded that volcanic ash emitted from Antarctic volcanoes could potentially encircle the globe, reaching South America and Africa. Moreover, they concluded that a Deception Island volcano eruption might lead to significant consequences for global aviation safety.

Anthropogenic fingerprints of long range atmospheric transport in the South Shetland Islands

One issue related to long-range atmospheric transport is the possibility of it being a means by which anthropogenic pollution reaches Antarctica, including the South Shetland Islands. This has been discussed by many authors, with varying conclusions (e.g. Bargagli et al. 1998; Graf et al. 2010; Kallenborn et al. 2013; McConnel et al. 2014; Szopińska et al. 2018). The difficulty in interpreting results stems from the fact that some elements and chemical compounds that are foreign to the Antarctic environment, such as heavy metals or PAHs, may come via long-range transport from remote continents, as well as from local factors – research stations or ship movements in this region (Martins et al. 2004; Curtosi et al. 2007; Bicego et al. 2009; Szopińska et al. 2016). This is the reason for drawing conclusions tentatively and identifying both possible areas (local and long-range) of source pollution.

However, the presence of some compounds, such as polychlorinated biphenyls (PCBs), attests to their reaching Antarctica by the atmospheric route from distant continents. The emission of PCBs ceased in the latter half of the 20th century, but these compounds are present in the Antarctic as the effect of earlier delivery by LRAT (Klánová et al. 2008). According to the map of organic compounds marked in the Antarctic environment (Potapowicz et al. 2019) PCBs are common in SSI. Many authors have described its occurrence in this area, in the soils

(Montone et al. 2001; Park et al. 2010; Cabrerizo et al. 2012, 2013), in the snow and air (Montone et al. 2003, 2005; Park et al. 2010; Cabrerizo et al. 2012, 2013; Li et al. 2012), in lichens (Montone et al. 2001; Cipro et al. 2010; Cabrerizo et al. 2012), in seabirds (Inomata et al. 1996; Montone et al. 2001; Corsolini et al. 2007; Schavione et al. 2009; Cipro et al. 2010; Corsolini et al. 2011; Jara-Carrasco et al. 2015; Mello et al. 2016) and in marine sediments and fauna (Montone et al. 2001; Cabrerizo et al. 2012; Lana et al. 2014).

Other anthropogenic compounds include Dichlorodiphenyldichloroethylene (DDTs), which have been indicated in many places across SSI (Potapowicz et al. 2019). DDTs were indicated in air (Montone et al. 2005), in sea birds (Inomata et al. 1996; Corsolini et al. 2007; Schavione et al. 2009; Taniguchi et al. 2009; Cipro et al. 2010; Corsolini et al. 2011; Jara-Carrasco et al. 2015), in fish tissues (Lana et al. 2014), in soils, lichens and mosses (Cabrerizo et al. 2012), and in lichens (Cipro et al. 2010).

According to Potapowicz et al. (2019) anthropogenic compounds are also indicated in other parts of Antarctica. However, it should be noted that the number of points with these pollutants in different parts of Antarctica are related to the availability of the area to researchers. The greatest numbers of sample points are found on the SSI, the Antarctic Peninsula, Ross Sea and Victoria Land, where numerous research stations operate. In selected places temporal observation of anthropogenic compounds was conducted. Kallenborn et al. (2013) indicated temporal changes in hexachlorocyclohexane and their derivatives (HCHs) in air samples in the area of the Norwegian Troll research station (Dronning Maud Land), and they associated changes in this pollutant's concentrations with its atmospheric transport from distant continents.

Some results also show the possibility of anthropogenic pollutants accumulating in ice, and indicate that changes in industrial lead contents (^{206}Pb/^{207}Pb isotopic ratios) in ice cores from the Antarctic and Antarctic Peninsula are connected with the industrial revolution (the late-18th century, when scientists had not yet reached the Antarctic) (McConnel et al. 2014). This connection is evidence of this pollution having arrived by an atmospheric

route. Moreover, the aforementioned authors pointed out that ice-core aerosol records show not only changes in emissions but also decadal and seasonal fluctuations – both in atmospheric circulation and long-range aerosol transport – from mid-to-low latitudes to the high southern latitudes.

Another potential source of pollution that can reach Antarctica by atmospheric means is the burning of biomass and uncontrolled fires on Southern Hemisphere continents. Hara et al. (2008) identified biomass burning in Africa and South America as the sources of seasonal variations in black carbon (BC) recorded at Syowa Station (Queen Maud Land). Pereira et al. (2006) indicated that the black carbon and total C time series in aerosols in the Ferraz station (King George Island, SSI) displayed relative increases in concentration during the winter-to-spring period in 1993, 1997 and 1998. According to these authors, these increases coincide with peak biomass burning in central South America, and are related to low-level anticyclonic circulation centred over the Atlantic Ocean resulting in large-scale continental outflow to the Atlantic Ocean, and also to cyclonic circulation over the extreme south of the South American continent. LRAT was also shown to be a source of black carbon on King George Island by Leal et al. (2008).

During the period under consideration (Sep 2015 – Aug 2017) there was a catastrophic fire lasting over a month that began on January 2nd 2017 in the vicinity of the village of Valparaíso (Chile); by the end of January it had consumed over 547,200 hectares (including 290,000 ha of forests). However, the analysis of air mass trajectories carried out in this work indicates that in January to February 2017 air masses flowed into the South Shetland Islands mainly from the Antarctic region (Table 2). Inflow from South America was recorded only on February 15. Moreover, the smoke plume from this wildfire was seen in satellite images (using the O3M SAF GOME-2 Absorbing Aerosol Index product) which confirmed the smoke plume's movement westwards over the Pacific Ocean (https://scienceblog. eumetsat.int/2017/02/observing-wildfire-smoke-plumes-from-space/). However, taking into account the significant frequency of fires in South America (Molina et al. 2015) and the high frequency of inflow of air masses to SSI from this area (Table 2, Figs 2

and 3), it can be concluded that the possibility of compounds from biomass combustion inflowing to the South Shetland Islands environment should not be ruled out.

Conclusions

The 731 air mass back trajectory studies conducted here confirm the possible long-range atmospheric transport of air masses to Antarctica (including the South Shetland Islands). The results show that air masses over SSI are shaped by the South Ocean during all days. However, for the study period of September 2015 to August 2017, the most common source area for air masses flowing in from outside Antarctica was South America. Therefore, we can conclude that South America is the most likely fetch area for the anhropogenic pollutants described described by many authors in the SSI area.

Moreover, taking into account that the western part of South America is one of the more active volcanic regions (historically and at present), based on the high frequency of air masses incoming from this direction, we can conclude that contaminants of volcanic origin marked in SSI may also have originated in the SA region, in addition to contaminants stored in the environment as the effect of Deception Island activity. Volcanic eruptions in particular (as well as sudden events related to human activities, such as large-scale forest fires) must coincide with air masses flowing into the Antarctic region in order for a "finger print" to be recorded in the environment. Therefore, it is advisable that short-term studies on the chemical composition of objects that change over time (such as surface waters, rainfall or snow) be compared with concurrent atmospheric inflows from outside Antarctica. When there has been a sudden event delivering large amounts of compounds into the atmosphere, results may vary considerably depending on whether such tests are carried out when there is no inflow of air masses from distant areas, or whether there is an inflow of air masses from the lower latitudes of the Southern Hemisphere at the time. Not taking this factor into account may lead to erroneous conclusions relating to the misinterpretation of their sources.

At the same time, due to the origin of some compounds being mixed – both natural and anthropogenic – there is a need to develop indicators that would take into account the coexistence and interdependence of anthropogenic compounds as well as allowing for an unambiguous interpretation of their origin.

Acknowledgements

References

ADAME J.A., VALENTÍ – PÍA M.D., GIL-OJEDA M., 2015, Impact evaluation of potential volcanic plumes over Spain. Atmospheric Research, 160: 39–49.

ARISTARAIN A.J., DELMAS R.J., 1998, Ice record of a large eruption of Deception Island Volcano (Antarctica) in the XVIIth century. Journal of Volcanology and Geothermal Research, 80: 17–25.

AYMERICH I.F., OLIVA M., GIRALT S., MARTÍN-HERRERO J., 2016, Detection of Tephra Layers in Antarctic Sediment Cores with Hyperspectral Imaging. PLoS ONE, 11(1): e0146578. doi:10.1371/journal.pone.0146578.

BARGAGLI R., SANCHEZ-HERNANDEZ J.C., MARTELLA L., MONACI F., 1998, Mercury, cadmium and lead accumulation in Antarctic mosses growing along nutrient and moisture gradients. Polar Biology, 19: 316–322.

BARGAGLI R., 2008, Environmental contamination in Antarctic ecosystems. Science of the Total Environment, 400: 212–26.

BENGTSON-NASH S., 2011, Persistent organic pollutants in Antarctica: Current and future research priorities. Journal of Environmental Monitoring, 13, 3: 497–504.

BENGTSON-NASH S., RINTOUL S.R., KAWAGUCHI S., STANILAND I., HOFF J., TIERNEY M., BOSSI R., 2010, Perfluorinated compounds in the Antarctic region: ocean circulation provides prolonged protection from distant sources. Environmental Pollution, 158: 2985–2991.

BICEGO M.C., LAMARDO M.Z., TANIGUCHI S., MARTINS C.C., DA SILVA D.A.M., SASAKI S.T., ALBERGARIA-BARBOSA A.C.R., PAOLO, F.S., WEBER, R.R., MONTONE, R.C., 2009, Results from a 15-year study on hydrocarbon concentrations in water and sediment from Admiralty Bay, King George Island, Antarctica. Antarctic Science, 21: 209–220.

BIRKENMAJER K., DELITALA M.C., NAREBSKI W., NICOLETTI M., PETRUCCIANI C., 1986, Geochronology and migration of Cretaceous through Tertiary plutonic centres, South Shetland Islands (West Antarctica): subduction and hot spot magmatism. Bulletin of the Polish Academy of Sciences, Earth Sciences, 34: 243–255.

BJÖRCK S., SANDGREN P., ZALE R., 1991, Late Holocene tephrochronology of the northern Antarctic Peninsula. Quaternary Research, 36: 322–328.

BOCKHEIM J., VIEIRA G., RAMOS M., LÓPEZ-MARTÍNEZ J., SERRANO E., GUGLIELMIN M., WILHELM K., NIEUWENDAM A., 2013., Climate warming and permafrost dynamics in the Antarctic Peninsula region. Global and Planetary Change, 100: 215–223.

CABRERIZO A., DACHS J., BARCELÓ D., JONES K.C., 2012, Influence of Organic Matter Content and Human Activities on the Occurrence of Organic Pollutants in Antarctic Soils, Lichens, Grass, and Mosses. Environmental Science and Technology, 46: 1396–1405.

CABRERIZO A., DACHS J., BARCELÓ D., JONES K.C., 2013, Climatic and Biogeochemical Controls on the Remobilization and Reservoirs of Persistent Organic Pollutants in Antarctica. Environmental Science and Technology, 47: 4299–4306.

CABRERIZO A., GALBÁN-MALAGÓN C., DELVENTO S., DACHS J., 2014, Sources and fate of polycyclic aromatic hydrocarbons in the Antarctic and South-

ern Ocean atmosphere. Global Biogeochemical Cycles, 28: 1424–1436, doi:10.1002/2014GB004910.

CHAMBERS S.D., HONG S.-B., WILLIAMS A.G., CRAWFORD J., GRIFFITHS A.D., PARK S.-J., 2014, Characterising terrestrial influences on Antarctic air masses using radon-222 measurements at King George Island. Atmospheric Chemistry and Physics Discussions, 14, 11541–11576.

CHEN B., STEIN A.F., MALDONADO P.G., SANCHEZ DE LA CAMPA A.M., GONZALEZ-CASTANEDO Y., CASTELL N., DE LA ROSA J.D., 2013, Size distribution and concentrations of heavy metals in atmospheric aerosols originating from industrial emissions as predicted by the HYSPLIT model. Atmospheric Environment, 71: 234–244.

CIPRO C.V.Z., TANIGUCHI S., MONTONE R.C., 2010, Occurrence of organochlorine compounds in Euphausia superba and unhatched eggs of Pygoscelis genus penguins from Admiralty Bay (King George Island, Antarctica) and estimation of biomagnification factors. Chemosphere, 78, 767–771.

CORSOLINI S., BORGHESI N., SCHIAMONE A., FOCARDI S., 2007, Polybrominated Diphenyl Ethers, Polychlorinated Dibenzo-dioxins, -furans, and -biphenyls in Three Species of Antarctic Penguins, Environmental Science and Pollution Research, 14(6): 421–429.

CORSOLINI S., 2009, Industrial contaminants in Antarctic biota. Journal of Chromatography A, 1216: 598–612.

CORSOLINI S., BORGHESI N., ADEMOLLO N., FOCARDI S., 2011, Chlorinated biphenyls and pesticides in migrating and resident seabirds from East and West Antarctica. Environment International, 37: 1329–1335.

CULOTTA L., GIANGUZZA A., MANNINO M.R., ORECCHIO S., 2007, Polycyclic aromatic hydrocarbons (PAHs) in Volcano Island (Aeollan Archipelago mud utilized for therapeutic purpose. Polycyclic Aromatic Compounds, 27: 281–294.

CURTOSI A., PELLETIER E., VODOPIVEZ C.L., MAC CORMACK W.P., 2007, Polycyclic aromatic hydrocarbons in soil and surface marine sediment near Jubany Station (Antarctica). Role of permafrost as a low-permeability barrier. Science of the Total Environment, 383: 193–204.

DAUNER A.L.L., HERNANDEZ E.A., MACCORMACK W.P., MARTINS C.C., 2015, Molecular characterisation of anthropogenic sources of sedimentary organic matter from Potter Cove, King George Island, Antarctica. Science of Total Environment, 502: 408–416.

DRAXLER R., STUNDER B., ROLPH G., STEIN A., TAYLOR A., 2009, HYSPLIT4 user's guide. Version 4.9. Silver Spring, MD: Air Resources Laboratory, National Oceanic and Atmospheric Administration.

DRAXLER R.R., ROLPH G.D., 2003, HYSPLIT (Hybrid Single-particle Lagrangian Integrated Trajectory). Air Resources Laboratory, National Oceanic and Atmospheric Administration. Model accessed at http://www.arl.noaa.gov/HYSPLIT.

DURANT A.J., VILLAROSA G., ROSE W.I., DELMELLE P., PRATA A.J., VIRAMONTE J.G., 2012, Long-range volcanic ash transport and fallout during the 2008 eruption of Chaitén volcano, Chile. Physics and Chemistry of the Earth, 45-46: 50-64.

HODGSON D.A., DYSON C.L, JONES V.J., SMELLIE J.L., 1998, Tephra analysis of sediments from Midge Lake (South Shetland Islands) and Sombre Lake (South Orkney Islands), Antarctica. Antarctic Science, 10 (1): 13–20.

EDWARDS D.P., EMMONS L.K., GILLE J.C., CHU A., ATTIE J.L., GIGLIO L., WOOD S.W., HAYWOOD J., DEETER M.N., MASSIE S.T., ZISKIN D.C., DRUMMOND J.R., 2006, Satellite-observed pollution from Southern Hemisphere biomass burning. Journal of Geophysical Research-Atmospheres, 111, D14: D14312, https://doi.org/10.1029/2005JD006655.

ESCUDERO M., STEIN A.F., DRAXLER R.R., QUEROL X., ALASTUEY A., CASTILLO S., AVILA A., 2011, Source apportionment for African dust outbreaks over the Western Mediterranean using the HYSPLIT model. Atmospheric Research, 99: 518–527.

FUOCO R., GIANNARELLI S., ONOR M., GHIMENTI S., ABETE C., TERMINE M., FRANCESCONI S., 2012, A snow/firn four-century record of polycyclic aromatic hydrocarbons (PAHs) and polychlorobipenyls (PCBs) at Talos Dome (Antarctica). Microchemical Journal, 105: 133–141.

GEYER A., MARTI A., GIRALT S., FOLCH A., 2017, Potential ash impact from Antarctic volcanoes: Insights from Deception Island's most recent eruption. Scientific Reports, 7: 16534, DOI:10.1038/s41598-017-16630-9.

GONZÁLEZ-FERRÁN O., 1991, The Bransfield rift and its active volcanism. [in:] Thomson M.R.A., Crame J.A., Thomson J.W. (eds), Geological Evolution of Antarctica. Cambridge University Press, Cambridge: 505–509.

GONZALEZ S., 2018, Atmospheric patterns over the Antarctic Peninsula. Journal of Climate, 31(9): 3597–3608.

GRAF H.E., FEICHTER J., LANGMANN B., 1997, Volcanic sulfur emissions – Estimates of source strength and its contribution to the global sulfate distribution. Journal of Geophysical Research, 102, D9: 10,727-10,738.

GRAF H.G., SHIRSAT S.V., OPPENHEIMER C., JARVIS M.J., PODZUN R., JACOB D., 2010, Continental scale Antarctic deposition of sulphur and black carbon from anthropogenic and volcanic sources. Atmospheric Chemistry and Physics, 10: 2457–2465.

HARA K., OSADA K., YABUKI M., HAYASHI M., YAMANOUCHI T., SHIOBARA M., WADA M., 2008, Measurement of black carbon at Syowa station, Antarctica: seasonal variation, transport processes and pathways. Atmospheric Chemistry and Physics Discussions, 8: 9883–9929.

INOMATA O.N.K., MONTONE R.C., LARA W.H., WEBER R.R., TOLEDO H.H.B., 1996, Tissue distribution of organochlorine residues – PCBs and pesticides – in Antarctic penguins. Antarctic Science, 8: 253–255.

JARA-CARRASCO S., GONZALEZ M., GONZALEZ-ACUNA D., CHIANG G., CELIS J., ESPEJO W., MATTALL P., BARRA R., 2015, Potential immunohaematological effects of persistent organic pollutants on chinstrap penguin. Antarctic Science, 27(4): 373–381.

JARMOŁOWICZ-SZULC K., KOZŁOWSKA A., 2016, Wulkanizm rejonu Auckland, Nowa Zelandia. Przegląd Geologiczny, 64: 101–104.

JONES D.A., SIMMONDS I.H., 1993, A climatology of southern hemisphere extratropical cyclones. Climate Dynamics, 9: 131–145.

KALLENBORN R., BREIVIK K., ECKHARDT S., LUNDER C.R., MANØ S., SCHLABACH M., STOHL A., 2013, Long-term monitoring of persistent organic pollutants (POPs) at the Norwegian Troll station in Dronning Maud Land, Antarctica. Atmospheric Chemistry and Physics, 13: 6983–6992.

KATALIN G., KÁROLY N., ULRIKE M., NELSON E., ZSOLT V., 2007, Boron concentrations of volcanic fields in different geotectonic settings. Journal of Volcanology and Geothermal Research, 159: 70–84.

KEJNA M., 1993, Types of atmospheric circulation in the region of H. Arctowski station (South Shetland Islands) in the years 1986-1989. Materiały XX Symp. Polarnego, Lublin: 369-378.

KEJNA M., LÁSKA K., 1999, Weather conditions at Arctowski Station, King George Island, South Shetland Islands, Antarctica in 1996. Polish Polar Research, 20(3): 203–220.

KLÁNOVÁ J., MATYKIEWICZOVÁ N., MÁČKA Z., PROŠEK P., LÁSKA K., KLÁN P., 2008, Persistent organic pollutants in soils and sediments from James Ross Island, Antarctica. Environmental Pollution, 152: 416-423.

KLÜSER L., ERBERTSEDER T., MEYER-ARNEK J., 2013, Observation of volcanic ash from Puyehue–Cordón Caulle with IASI. Atmospheric Measurement Techniques, 6: 35–46.

KOZAK K., RUMAN M., KOSEK K., KARASIŃSKI G., STACHNIK Ł., POLKOWSKA Ż., 2017, Impact of Volcanic Eruptions on the Occurrence of PAHs Compounds in the Aquatic Ecosystem of the Southern Part of West Spitsbergen (Hornsund Fjord, Svalbard). Water, 9, 1: 42.

LANA N.B., BERTON P., COVACI A., CIOCCOB N.F., BARRERA-ORO E., ATENCIO A., ALTAMIRANO J.C., 2014, Fingerprint of persistent organic pollutants in tissues of Antarctic notothenioid fish. Science of the Total Environment, 499: 89–98.

LARA M., CARDONA A., MONSALVE G., YARCE J., MONTES C., VALENCIA V., WEBER M., DE LA PARRA F., ESPITIA D., LÓPEZ-MARTÍNEZ M., 2013, Middle Miocene near trench volcanism in northern Colombia: A record of slab tearing due to the simultaneous subduction of the Caribbean Plate under South and Central America. Journal of South American Earth Sciences, 45: 24–41.

LEAL M.A., JOPPERT M., LICÍNIO M.V., EVANGELISTA H., MALDONADO J., DALIA K.C., LIMA C., BARROS LEITE C.V., CORREA S.M., MEDEIROS G., DIAS DA CUNHA K., 2008, Atmospheric Impacts due to Anthropogenic Activities in Remote Areas: The Case Study of Admiralty Bay/King George Island/Antarctic Peninsula. Water, Air, and Soil Pollution, 188: 67–68.

LEAT P.T., DAY S.J., TATE A.J., MARTIN T.J., OWEN M.J., TAPPIN D.R., 2013, Volcanic evolution of the South Sandwich volcanic arc, South Atlantic, from multibeam bathymetry. Journal of Volcanology and Geothermal Research, 265: 60–77.

LEE Y.I., LIM H.S., YOON I., 2004, Geochemistry of soils of King George Island, South Shetland Islands, West Antarctica: Implications for pedogenesis in cold

polar regions. Geochimica et Cosmochimic Acta, 68(21): 4319–4333.

LEE Y.I., LIM H.S., YOON H.I., TATUR A., 2007, Characteristics of tephra in Holocene lake sediments on King George Island, West Antarctica: implications for deglaciation and paleoenvironment. Quaternary Science Reviews, 26, 25: 3167–3178.

LE MASURIER W.E., THOMSON J.W., BAKER P.E., KYLE P.R., ROWLEY P.D., SMELLIE J.L., VERWOERD W.J (eds), 1990, Volcanoes of the Antarctic Plate and Southern Oceans. Antarctic Research Series, American Geophysical Union.

LI Y., GENG D., LIU F., WANG T., ZHANG Q., JIANG H., 2012, Study of PCBs and PBDEs in King George Island, Antarctica, using PUF passive air sampling. Atmospheric Environment, 51: 140–145.

LIU E.J., OLIVA M., ANTONIADES D., GIRALT S., GRANADOS I., PLA-RABES S., Toro M., Geyer A., 2016, Expanding the tephrochronological framework for Byers Peninsula, Antarctica, by combined compositional and textural fingerprinting. Sedimentary Geology, 340: 49–61.

MARTINS C.C., BICEGO M.C., TANIGUCHI S., MOTONE R.C., 2004, Aliphatic and polycyclic aromatic hydrocarbons in surface sediments in Admiralty Bay, King George Island, Antarctica. Antarctic Science, 16(2): 117–122.

MATTIOLI G.S., LA FEMINA P.C., 2016, Final Report submitted to the National Science Foundation, Community Workshop: Scientific Drivers and Future of Mount Erebus Volcano Observatory (MEVO), https://www.unavco.org/community/meetings-events/2016/mevo/2016-MEVO-Final-Report.pdf).

McCONNELL J.R., MASELLI O.J., SIGL M., VALLELONGA P., NEUMANN T., ANSCHÜTZ H., BALES R.C., CURRAN M.A.J., DAS S.B., EDWARDS R., KIPFSTUHL S., LAYMAN L., THOMAS E.R., 2014, Antarctic-wide array of high-resolution ice core records reveals pervasive lead pollution began in 1889 and persists today. Scientific Reports, 4: 5848, DOI: 10.1038/srep05848.

McGOWAN H., CLARK A., 2008, Identification of dust transport pathways from Lake Eyre, Australia using Hysplit. Atmospheric Environment, 42: 6915–6925.

MELLO F.V., ROSCALES J.L., GUIDA Y.S., MENEZES J.F.S., VICENTE A., COSTA E.S., JIMÉNEZ B., TORRES J.P.M., 2016, Relationship between legacy and emerging organic pollutants in Antarctic seabirds and their foraging ecology as shown by $\delta^{13}C$ and $\delta^{15}N$. Science of the Total Environment, 573: 1380–1389.

MISHRA V.K., KIM K.H., HONG S., LEE K., 2004, Aerosol composition and its sources at the King Sejong Station, Antarctic Peninsula. Atmospheric Environment, 38: 4069–4084.

MOLINA L.T., GALLARDO L., ANDRADE M., BAUMGARDNER D., BORBOR-CÓRDOVA M., BÓRQUEZ R., CASASSA G., CERECEDA-BALI F., DAWIDOWSKI L., GARREAUD R., HUNEEUS N., LAMBERT F., MCCARTY J.L., PHEE J.M.C, MENA-CARRASCO M., RAGA G.B., SCHMITT C., SCHWARZ J.P., 2015, Pollution and its impacts on the South American Cryosphere. Earth's Future, 3: 345–369.

MONTONE R.C., TANIGUCHI S., WEBER R.R., 2001, Polychlorinated Biphenyls in Marine Sediments of Admiralty Bay, King George Island. Marine Pollution Bulletin, 42: 611–614.

MONTONE R.C., TANIGUCHI S., WEBER R.R., 2003, PCBs in the atmosphere of King George Island, Antarctica. Science of the Total Environment, 308: 167–173.

MONTONE R.C., WEBER R.R., TANIGUCHI S., 2005, PCBs and chlorinated pesticides (DDTs, HCHs and HCB) in the atmosphere of the southwest Atlantic and Antarctic oceans. Marine Pollution Bulletin, 50: 778–782.

OLIVA M., NAVARRO F., HRBÁČEK F., HERNÁNDEZ A., NÝVLT D., PEREIRA P., RUIZ-FERNÁNDEZ J., TRIGO R., 2017, Recent regional climate cooling on the Antarctic Peninsula and associated impacts on the cryosphere. Science of the Total Environment, 580: 210–223.

PARK H., LEE S.H., KIM M., KIM J.H., LIM H.S., 2010, Polychlorinated biphenyl congeners in soils and lichens from King George Island, South Shetland Islands, Antarctica. Antarctic Science, 22(01): 31–38.

PEDRAZZI D., AGUIRRE-DÍAZ G., BARTOLINI S., MARTÍ J., GEYER A., 2014, The 1970 eruption on Deception Island (Antarctica): eruptive dynamics and implications for volcanic hazards. Journal of the Geological Society, 171(6): 765–778.

PEREIRA E.B., EVANGELISTA H., PEREIRA K.C.D., CAVALCANTI I.F.A., SETZER A.W., 2006, Apportionment of black carbon in the South Shetland Islands, Antarctic Peninsula. Journal of Geophysical Research, 111, D03303, doi:10.1029/2005JD006086.

POTAPOWICZ J., SZUMIŃSKA D., SZOPIŃSKA M., POLKOWSKA Ż., 2019, The influence of glob-

al climate change on the environmental fate of anthropogenic pollution released from the permafrost Part I. Case study of Antarctica. Science of the Total Environment, 651: 1534-1548, doi:10.1016/j.scitotenv.2018.09.168.

PUNSOMPONGA P., CHANTARA S., 2018, Identification of potential sources of PM10 pollution from biomass burning in northern Thailand using statistical analysis of trajectories. Atmospheric Pollution Research, 9(6): 1038-1051, doi.org/10.1016/j.apr.2018.04.003.

RAGA G.B., BAUMGARDNER D., MAYOL-BRACERO O.L., 2016, History of Aerosol-Cloud Interactions Derived from Observations in Mountaintop Clouds in Puerto Rico. Aerosol and Air Quality Research, 16: 674–688.

RAVINDRA K., SOKHI R., VAN GRIEKEN R., 2008, Atmospheric polycyclic aromatic hydrocarbons: Source attribution, emission factors and regulation. Atmospheric Environment, 42: 2895–2921.

RUSSELL A., McGREGOR G.R., 2010, Southern hemisphere atmospheric circulation: impacts on Antarctic climate and reconstructions from Antarctic ice core data. Climatic Change, 99: 155–192.

SADYŚ M., KENNEDY R., SKJØTH C.A., 2015, An analysis of local wind and air mass directions and their impact on Cladosporium distribution using HYSPLIT and circular statistics. Fungal Ecology, 18: 56–66.

SALMON M., KENNETT B.L.N., STERN T., AITKEN A.R.A., 2013, The Moho in Australia and New Zealand. Tectonophysics, 609: 288–298.

SCHIAVONE A., CORSOLINI S., BORGHESI N., FOCARDI S., 2009, Contamination profiles of selected PCB congeners, chlorinated pesticides, PCDD/Fs in Antarctic fur seal pups and penguin eggs. Chemosphere, 76: 264–269.

SHAHID I., KISTLER M., MUKHTAR A., GHAURI B.M., RAMIREZ-SANTA CRUZ C., BAUER H., PUXBAUM H., 2016, Chemical characterization and mass closure of PM10 and PM2.5 at an urban site in Karachi – Pakistan. Atmospheric Environment, 128: 114–123.

SIMMONDS I., KEAY K., 2000, Variability of Southern Hemisphere Extratropical Cyclone Behavior, 1958–97. Journal of Climate, 13: 550–561.

STRACQUADANIO M., DINELLIB E., TROMBINI C., 2003, Role of volcanic dust in the atmospheric transport and deposition of polycyclic aromatic hydrocarbons and mercury. Journal of Environmental Monitoring, 5:984–988

SZOPIŃSKA M., NAMIEŚNIK J., POLKOWSKA Ż., 2016, How Important is Research on Pollution Levels in Antarctica? Historical Approach, Difficulties and Current Trends. Reviews of Environmental Contamination and Toxicology, 239: 79–156.

SZOPIŃSKA M., SZUMIŃSKA D., BIALIK R.J., CHMIEL S., PLENZLER J., POLKOWSKA Ż., 2018, Impact of a newly-formed periglacial environment and other factors on fresh water chemistry at the western shore of Admiralty Bay in the summer of 2016 (King George Island, Maritime Antarctica). Science of the Total Environment, 613–614: 619–634.

TANIGUCHI S., MONTONE R.C., BÍCEGO M.C., COLABUONO F.I., WEBER R.R., SERICANO J.L., 2009, Chlorinated pesticides, polychlorinated biphenyls and polycyclic aromatic hydrocarbons in the fat tissue of seabirds from King George Island, Antarctica. Marine Pollution Bulletin, 58: 129–133.

TATUR A., DEL VALLE R., BARCZUK A., 1999, Discussion on the uniform pattern of Holocene tephrochronology in South Shetland Islands, Antarctica. POLISH POLAR STUDIES. Institute of Ecology, 26 Polar Symposium: 303–321.

TURNER J., COLWELL S.R., MARSHALL G.J., LACHLAN-COPE T.A., CARLETON A.M., JONES P.D., LAGUN V., REID P.A., LAGOVKIN S., 2005, Antarctic climate change during the last 50 years. International Journal of Climatology, 25: 279–294.

TURNER J., LU H., WHITE I., KING J.C., PHILLIPS T., SCOTT HOSKING J., BRACEGIRDLE T.J., MARSHALL G.J., MULVANEY R., DEB P., 2016, Absence of 21st century warming on Antarctic Peninsula consistent with natural variability. Nature 535: 411–423, doi:10.1038/nature18645.

VAN DROOGE B.L., FERNÁNDEZ P., GRIMALT J.O., STUCHLÍK E., GARCÍA C.J.T., CUEVAS E., 2010, Atmospheric polycyclic aromatic hydrocarbons in remote European and Atlantic sites located above the boundary mixing layer. Environmental Science and Pollution Research, 17: 1207–1216.

VAN WYK DE VRIES M., BINGHAM R.G., HEIN A.S., 2018, A new volcanic province: an inventory of subglacial volcanoes in West Antarctica. [in:] Siegert M.J., Jamieson S.S.R., White D.A. (eds), Exploration of Subsurface Antarctica: Uncovering Past Changes and Modern Processes. Geological Society, Lon-

don, Special Publications, 461, https://doi.org/10.1144/SP461.7

VAUGHAN D.G., MARSHALL G.J., CONNOLLEY W.M., PARKINSON C., MULVANEY R., HODGSON D.A., KING J.C., PUDSEY C.J., TURNER J., 2003, Recent rapid regional climate warming on the Antarctic Peninsula. Climate Change, 60: 243–274.

VIEIRA G., LÓPEZ-MARTÍNEZ J., SERRANO E., RAMOS M., 2008, Climate change and permafrost degradation. Geomorphological evidence from Deception and Livingston islands, maritime Antarctic. [in:] Kane, D.L., Hindel, K.M. (eds), Proceedings Ninth International Conference on Permafrost. 2. Institute of Northern Engineering, University of Alaska, Fairbanks: 1839–1844.